Eur. Phys. J. C 20, 1–11 (2001)
Digital Object Identifier (DOI) 10.1007/s100520100646

THE EUROPEAN PHYSICAL JOURNAL C

4-Neutrino mass schemes and the likelihood of (3+1)-mass spectra

W. Grimus[a], T. Schwetz[b]

Universität Wien, Institut für Theoretische Physik, Boltzmanngasse 5, 1090 Wien, Austria

Received: 26 February 2001 /
Published online: 25 April 2001 –

Abstract. We examine the (3+1)-class of 4-neutrino mass spectra within a rigorous statistical analysis based on the Bayesian approach to probability. The data of the Bugey, CDHS and KARMEN experiments are combined by using a likelihood function. Our statistical approach allows us to incorporate solar and atmospheric neutrino data and also the result of the CHOOZ experiment via inequalities which involve elements of the neutrino mixing matrix and are derived from these data. For any short-baseline Δm^2 we calculate a bound on the LSND transition amplitude $A_{\mu;e}$ and find that, in the Δm^2–$A_{\mu;e}$ plane, there is no overlap between the 99% CL region allowed by the latest LSND analysis and the region allowed by our bound on $A_{\mu;e}$ at 95% CL; there are some small overlap regions if we take the bound at 99% CL. Therefore, we conclude that, with the existing data, the (3+1)-neutrino mass spectra are not very likely. However, treating the (2+2)-spectra with our method, we find that they are well compatible with all data.

1 Introduction

At present, there are three indications in favour of neutrino oscillations [1], namely the solar ν_e deficit [2], the atmospheric $\overset{(-)}{\nu}_\mu$ [3,4] deficit and the result of the LSND experiment [5,6] hinting at $\overset{(-)}{\nu}_\mu \to \overset{(-)}{\nu}_e$ transitions. Whereas in the case of the first two indications several experiments agree on the existence of the effect, the third indication is found only by the LSND collaboration. Therefore, in many analyses the LSND result is left out. However, if all three indications in favour of neutrino oscillations are confirmed, for three mass-squared differences of different orders of magnitude ($10^{-10}\,\mathrm{eV}^2 < \Delta m^2_{\mathrm{solar}} < 10^{-7}\,\mathrm{eV}^2$ or $\Delta m^2_{\mathrm{solar}} \sim 10^{-5}\,\mathrm{eV}^2$, $\Delta m^2_{\mathrm{atm}} \sim 3 \times 10^{-3}\,\mathrm{eV}^2$, $\Delta m^2_{\mathrm{LSND}} \sim 1\,\mathrm{eV}^2$) one needs a minimum of four neutrinos, three active ones and a sterile one [7]. In that case a major revision of our picture of the lepton sector of the elementary particles would be necessary, with a mixing between the active and the sterile neutrinos; i.e.,

$$\nu_{\alpha\mathrm{L}} = \sum_{j=1}^{4} U_{\alpha j} \nu_{j\mathrm{L}} \quad \text{with} \quad \alpha = e, \mu, \tau, s, \tag{1}$$

if we stick to the minimum of four neutrinos. In (1) the left-handed flavour fields are denoted by $\nu_{\alpha\mathrm{L}}$ and the left-handed mass eigenfields by $\nu_{j\mathrm{L}}$, and the 4×4 neutrino mixing matrix U is assumed to be unitary.

One of the most important issues in the context of 4-neutrino scenarios is the question of the 4-neutrino mass spectrum [8–10]. There are two different spectral classes with very different properties: the first class contains four types and consists of spectra where three neutrino masses are clustered together, whereas the fourth mass is separated from the cluster by the mass gap needed to reproduce the LSND result[1]; the second class has two types where two pairs of nearly degenerate masses are separated by the LSND gap. These two classes have been dubbed (3+1) and (2+2)-neutrino mass spectra, respectively [11]. The main difference between these two classes is that, if a (2+2)-spectrum is realised in nature, the transition into the sterile neutrino is a solution of either the solar or the atmospheric neutrino problem, or the sterile neutrino has to take part in both, whereas with a (3+1)-spectrum it could be only slightly mixed with the active neutrinos and mainly provide a description of the LSND result.

It has been argued in the literature [8–10,12] that the (3+1)-spectra are strongly disfavoured by the data, whereas the (2+2)-spectra are the preferred ones, in agreement with all data showing evidence for neutrino oscillations and also with those where no such evidence has been found. Recently, in [11,13,14] this statement has been challenged because in the latest LSND analysis the allowed region in the Δm^2–$A_{\mu;e}$ plane, where $A_{\mu;e}$ is the LSND transition amplitude, has undergone a slight shift towards smaller mass-squared differences, which makes the (3+1)-spectra somewhat less disfavoured. Furthermore, in a 2-

[a] e-mail: grimus@doppler.thp.univie.ac.at
[b] e-mail: schwetz@doppler.thp.univie.ac.at

[1] This class contains the hierarchical mass spectrum

neutrino analysis of atmospheric neutrino oscillations the Super-Kamiokande data prefer $\nu_\mu \to \nu_\tau$ conversion over $\nu_\mu \to \nu_s$ [15]. Moreover, there is some debate also on the solar neutrino problem: the issue is whether the $\nu_e \to \nu_s$ transition is disfavoured in comparison with other solutions [16], though such a feature seems not to be borne out by a global analysis of the data [17]. In any case, moving away from pure 2-neutrino considerations in the solar and atmospheric neutrino problems, transitions into active–sterile superpositions [18,19] give viable solutions to both problems within the (2+2)-spectral schemes, with features which will be tested in the future [14].

The arguments presented in [8–10], which disfavour the (3+1)-mass spectra, are based on exclusion curves from short-baseline (SBL) experiments, and solar and atmospheric neutrino data enter into this simplified analysis only through inequalities. The advantage of this approach is that its parameters are confined to the quantities[2]

$$d_\alpha = |U_{\alpha 4}|^2 \quad (\alpha = e, \mu) \tag{2}$$

and the SBL or LSND mass-squared difference Δm^2. For definiteness we assume that the mass separated by the LSND gap is m_4 and, therefore, $\Delta m^2 = |m_4^2 - m_1^2|$. It has turned out that the up–down asymmetry of atmospheric multi-GeV μ-like events measured in the Super-Kamiokande experiment [3] is very suitable to constrain d_μ [10], whereas from the solar data it follows that d_e must be small. The probability of SBL $\nu_\mu \to \nu_e$ transitions is given by the two-neutrino-like formula [8]

$$P_{\nu_\mu \to \nu_e} = P_{\bar\nu_\mu \to \bar\nu_e} = A_{\mu;e} \sin^2 \frac{\Delta m^2 \mathrm{L}}{4E}, \tag{3}$$

where L is the distance between source and detector and E is the neutrino energy and

$$A_{\mu;e} = 4 d_e d_\mu. \tag{4}$$

The LSND experiment gives an allowed region in the Δm^2–$A_{\mu;e}$ plane.

However, the arguments of [8–10] are not based on a well-defined statistical procedure. Therefore, they remain on a semi-quantitative level and do not allow one to assess a confidence level (CL) which quantifies the degree at which the (3+1)-spectra are excluded.

In this paper we make a step forward towards such an assessment. The main points to achieve our goal are the following:

(1) The aim is to arrive, for every SBL mass-squared difference Δm^2, at a probability distribution solely in terms of d_e and d_μ; a suitable method for this purpose is given by the likelihood function in combination with the Bayesian approach (see, e.g., [20,21]).
(2) We make full use of the data of the SBL Bugey [23], CDHS [25] and KARMEN [26,27] experiments through the likelihood function.
(3) In the spirit of [8,10], all information pertaining to the atmospheric and solar mass-squared differences is included via inequalities. Within our probabilistic framework we are able to treat inequalities as prior probabilities or with a kind of a maximum likelihood method.
(4) In this way we treat the inequality following from the atmospheric up–down asymmetry and, similarly, we include also the result of the CHOOZ experiment [22]; the solar neutrino data allow a simpler treatment in the context of the Bugey data [23], as described in [8,24].
(5) Eventually, for every given SBL Δm^2 and any CL β, we are able to calculate an upper bound $A^0_\beta(\Delta m^2)$ on the transition amplitude $A_{\mu;e}$, and we can compare such bounds $A^0_\beta(\Delta m^2)$ with the 90% and 99% CL regions in the Δm^2–$A_{\mu;e}$ plane found by the LSND experiment [6].

In the same framework we will also discuss the (2+2)-spectra.

The plan of the paper is as follows. In Sect. 2 we rederive the atmospheric up–down inequality [10] in a form which is suitable for our purpose. In Sect. 3 we introduce the likelihood function and the Bayesian approach, and describe how to incorporate inequalities; we apply the methods developed there to the CHOOZ result and the atmospheric up–down inequality. In Sect. 4 we explain how we calculate bounds on $A_{\mu;e}$ and discuss each of the SBL experiments we use, together with their features which are important in this context. Details of a technical nature are deferred to the appendix. Our main result, represented as a plot in the Δm^2–$A_{\mu;e}$ plane, is also given in this section. In Sect. 5 we consider the (2+2)-spectra in the framework of our statistical approach and in Sect. 6 we draw our conclusions.

2 The atmospheric up–down asymmetry as a constraint on short-baseline neutrino oscillations

The most convincing evidence for $\overset{(-)}{\nu}_\mu$ disappearance in atmospheric neutrino experiments is given by the so-called up–down asymmetry

$$A_{\mathrm{ud}} = \frac{U - D}{U + D} \tag{5}$$

measured by the Super-Kamiokande Collaboration [3], where U and D refer to the number of up-going and down-going μ-like multi-GeV events, respectively. Quoting the number for fully contained events, after 1289 days of operation the result

$$A^{\mathrm{exp}}_{\mathrm{ud}} = -0.327 \pm 0.045 \pm 0.004 \tag{6}$$

was found [28]. Adding statistical and systematic error in quadrature, one obtains

$$\Delta A^{\mathrm{exp}}_{\mathrm{ud}} \equiv \sigma_A = 0.045. \tag{7}$$

Because of the smallness of the systematic error this value is identical with the statistical error.

Let us now rederive the atmospheric up–down inequality [10]. In the following we will not indicate antineutrinos but our arguments will hold for both, neutrinos and

[2] Note that in [10] the quantities $c_\alpha = 1 - d_\alpha$ are used instead

antineutrinos. With the assumption that downward-going atmospheric neutrinos do not oscillate with the frequency associated with $\Delta m^2_{\rm atm}$ and that oscillations according to Δm^2 are averaged out, we obtain

$$P^D_{\nu_\mu\to\nu_\mu} = d_\mu^2 + (1-d_\mu)^2 \quad \text{and} \quad P^D_{\nu_e\to\nu_\mu} = \frac{1}{2}A_{\mu;e}. \quad (8)$$

Denoting the number of muon (electron) neutrinos and antineutrinos produced in the atmosphere by n_μ (n_e), it follows from (8) that

$$D = n_\mu[d_\mu^2 + (1-d_\mu)^2] + \frac{1}{2}n_e A_{\mu;e}. \quad (9)$$

For the upward-going neutrinos we have the inequalities [10]

$$P^U_{\nu_\mu\to\nu_\mu} \geq d_\mu^2 \quad \text{and} \quad P^U_{\nu_e\to\nu_\mu} \geq \frac{1}{4}A_{\mu;e}. \quad (10)$$

We, therefore, have the inequality

$$U \geq n_\mu d_\mu^2 + \frac{1}{4}n_e A_{\mu;e}. \quad (11)$$

Note that for the (3+1)-spectra the amplitude $A_{\mu;e}$ is given by (4). Since $-A_{\rm ud}$ (5) is a monotonously decreasing function in U, using (9) and (11) we obtain the so-called up–down inequality for μ-like atmospheric events

$$-A_{\rm ud} \leq G(d_e, d_\mu) = \frac{(1-d_\mu)^2 + d_e d_\mu/r}{(1-d_\mu)^2 + 2d_\mu^2 + 3d_e d_\mu/r}. \quad (12)$$

In this equation we have defined $r = n_\mu/n_e$. The numerical value $r \simeq 2.8$ can be read off from Fig. 3 in [3] of the Super-Kamiokande Collaboration. With similar arguments one can also find an upper bound

$$A_{\rm ud} \leq H(d_e, d_\mu) = \frac{d_\mu(1-d_\mu) - d_e d_\mu/r}{1 - d_\mu(1-d_\mu) + d_e d_\mu/r}. \quad (13)$$

Hence, the up–down asymmetry is confined to the interval

$$-G \leq A_{\rm ud} \leq H. \quad (14)$$

Some remarks are at order. Our inequality (12) is a little different from the analogous inequality in [10], because in the present case we have not eliminated d_e; this is useful because our aim is to derive a probability distribution in d_e and d_μ (see next section). The ratio r has a slight dependence on the atmospheric zenith angle which is neglected here; however, since d_e is confined to rather small values [8, 24] by the result of the Bugey experiment [23], the terms containing r are rather unimportant numerically. The assumptions for deriving (12) and (13) are not exactly fulfilled: for down-going neutrinos with zenith angles around 0°, oscillations according to small SBL mass-squared differences Δm^2 around $0.2\,\mathrm{eV}^2$ are not completely averaged out; for down-going neutrinos with zenith angles close to 90°, oscillations according to $\Delta m^2_{\rm atm}$ do occur already, if the atmospheric mass-squared difference is large. We have checked that both effects do not change numerically the bound G by more than a few percent in the worst case. Finally, matter effects, which are important for up-going neutrinos, do not affect the inequalities (10) and thus also not the inequality for U. Formula (12) is, therefore, a well-established inequality which restricts mainly the allowed range of d_μ. Due to (4), it will be used in the following to constrain the SBL amplitude $A_{\mu;e}$.

3 The statistical treatment of inequalities

As mentioned in the introduction, a suitable method for the purpose of deriving a probability distribution in the variables d_e and d_μ is given by the likelihood function combined with the Bayesian approach, which is defined as follows. Suppose one has a series of measurements $x = (x_1, \ldots, x_n)$ and r parameters $\theta = (\theta_1, \ldots, \theta_r)$ to be estimated. Then the Bayesian approach allows to construct a "posterior" probability density in the parameter space via (see, e.g., [20,21])

$$p(\theta|x) = \frac{L(x|\theta)\pi(\theta)}{\int \mathrm{d}^r\theta' L(x|\theta')\pi(\theta')}. \quad (15)$$

In this expression, $L(x|\theta)$ is the likelihood function and $\pi(\theta)$ is the prior probability density associated with the parameters θ, reflecting the state of knowledge of θ before the measurement.

3.1 Inequalities included as priors

Let us suppose now that we consider an observable Z whose experimental value is $z_{\rm exp} \pm \sigma_z$ and its *true* value is z. We assume that the values of measurements of Z are distributed according to a Gaussian distribution

$$L_Z = \frac{1}{\sqrt{2\pi}\sigma_z}\exp\left[-\frac{1}{2}\left(\frac{z_{\rm exp}-z}{\sigma_z}\right)^2\right] \quad (16)$$

around the true value. Suppose further that from some theoretical consideration we have the knowledge that the true value z is bounded by

$$a \leq z \leq b. \quad (17)$$

We conceive of the true value z, which is otherwise unknown, as a parameter in our scenario and assign to it a prior probability density

$$\pi_Z(z) = \frac{1}{b-a}\Theta(b-z)\Theta(z-a), \quad (18)$$

where Θ denotes the Heaviside function. Due to lack of further knowledge, we have assumed a flat prior probability density. Since we are not interested in a posterior probability density in the parameter z we perform the integral

$$\int \mathrm{d}z L_Z(z)\pi_Z(z) = \ell_Z \quad (19)$$

with

$$\ell_Z = \frac{1}{2(b-a)} \left\{ \mathrm{erf}\left(\frac{b - z_{\mathrm{exp}}}{\sqrt{2}\sigma_z} \right) + \mathrm{erf}\left(\frac{z_{\mathrm{exp}} - a}{\sqrt{2}\sigma_z} \right) \right\}, \tag{20}$$

where we have made use of the error function defined by

$$\mathrm{erf}(z) = \frac{2}{\sqrt{\pi}} \int_0^z \mathrm{d}t \mathrm{e}^{-t^2}. \tag{21}$$

The function (20) represents then the relevant factor in the posterior probability density which takes into account the inequality (17).

To check if we have been lead to a meaningful expression (20), we want to discuss the behaviour of this function. Following from $\mathrm{erf}(\infty) = -\mathrm{erf}(-\infty) = 1$, we find that for $a \ll z_{\mathrm{exp}} \ll b$ we have $\ell_Z \simeq 1/(b-a)$ to a very good approximation, and for $z_{\mathrm{exp}} \gg b$ or $z_{\mathrm{exp}} \ll a$ we have $\ell_A \simeq 0$. In this discussion, "much smaller" or "much larger" is defined in units of σ_z. If we assume that σ_z becomes negligibly small, the function ℓ_Z approaches a step function with $1/(b-a)$ being the height of the step. The edges of the step are smoothened out by a finite σ_z. Thus, we will have a maximal contribution to the posterior probability density for z_{exp} well inside the interval $[a, b]$, whereas for z_{exp} well outside the interval $[a, b]$ the function ℓ_Z is very close to zero. Thus we can be confident that the inequality (17) is reasonably well taken into account by our procedure.

3.2 Inequalities treated with a maximum likelihood method

Again we start from (16) and (17). Now we take into account our lack of knowledge about the true value of Z by maximising L_Z as a function of $z \in [a, b]$. It is easy to check that one obtains

$$\begin{aligned} \max_{z \in [a,b]} L_Z &\equiv L_Z^m \\ &= \frac{1}{\sqrt{2\pi}\sigma_z} \exp\left\{ -\frac{1}{2} \left[\left(\frac{z_{\mathrm{exp}} - b}{\sigma_z} \right)^2 \Theta(z_{\mathrm{exp}} - b) \right.\right. \\ &\quad \left.\left. + \left(\frac{a - z_{\mathrm{exp}}}{\sigma_z} \right)^2 \Theta(a - z_{\mathrm{exp}}) \right] \right\}. \end{aligned} \tag{22}$$

In Appendix A we will discuss how this method is related to the method in the previous section.

3.3 The treatment of the CHOOZ result and the atmospheric up–down inequality in our statistical approach

The CHOOZ experiment is a long-baseline $\bar{\nu}_e$ disappearance experiment. It measures the survival probability P_{CH}, for which we derive the inequality

$$\begin{aligned} P_{\mathrm{CH}} &= 1 - 2d_e(1-d_e) \\ &\quad - 2|U_{e3}|^2(1 - d_e - |U_{e3}|^2)(1 - \cos\phi_{\mathrm{atm}}) \\ &\leq 1 - 2d_e(1-d_e). \end{aligned} \tag{23}$$

We have used the abbreviation $\phi_{\mathrm{atm}} = \Delta m^2_{\mathrm{atm}} L/2E$. We consider P_{CH} in (23) as the *true* survival probability, as opposed to the experimental value $P_{\mathrm{CH}}^{\mathrm{exp}} = 1.01$ with the error $\sigma_{\mathrm{CH}} = 0.039$ [22]. Thus we have the range

$$0 \leq P_{\mathrm{CH}} \leq 1 - 2d_e(1-d_e). \tag{24}$$

Making the substitutions

$$\begin{aligned} &a \to 0, \quad b \to 1 - 2d_e(1-d_e), \quad z \to P_{\mathrm{CH}}, \\ &z_{\mathrm{exp}} \to P_{\mathrm{CH}}^{\mathrm{exp}}, \quad \sigma_z \to \sigma_{\mathrm{CH}}, \end{aligned} \tag{25}$$

the CHOOZ result can be included in the statistical analysis according to both methods described in the previous subsections.

For the atmospheric up–down inequality we substitute

$$\begin{aligned} &a \to -G, \quad b \to H, \quad z \to A_{\mathrm{ud}}, \\ &z_{\mathrm{exp}} \to A_{\mathrm{ud}}^{\mathrm{exp}}, \quad \sigma_z \to \sigma_A, \end{aligned} \tag{26}$$

where G, H, $A_{\mathrm{ud}}^{\mathrm{exp}}$ and σ_A are given by (12), (13), (6) and (7), respectively. Notice that, since we have $A_{\mathrm{ud}}^{\mathrm{exp}} \ll 0$ and $H \geq 0$, the first term in the exponential of the expression (22) does not contribute here, and the first term in the expression (20) is 1 for all practical purposes.

The substitutions (25) and (26) allow us to define – according to (16), (18), (20), (22) – the functions L_{CH}, π_{CH}, ℓ_{CH}, L_{CH}^m and L_{ud}, π_{ud}, ℓ_{ud}, L_{ud}^m, referring to the CHOOZ experiment and the atmospheric up–down inequality, respectively. These functions will be used in the following discussions.

4 A bound on the LSND $\overset{(-)}{\nu}_\mu \to \overset{(-)}{\nu}_e$ transition amplitude

4.1 The statistical procedure

Let us now describe how to derive our desired probability distribution. We concentrate on the four parameters d_e, d_μ, A_{ud} and P_{CH}. We want to stress again that the latter two quantities are conceived of as *true* values. Therefore, they are parameters within our procedure and we will treat them according to the methods described in Sect. 3, in order to arrive at a distribution solely in d_e and d_μ. The likelihood function is given by

$$L = L_{\mathrm{osc}}(d_e, d_\mu) \times L_{\mathrm{ud}}(A_{\mathrm{ud}}) \times L_{\mathrm{CH}}(P_{\mathrm{CH}}), \tag{27}$$

where the first factor L_{osc} is the product of the likelihood functions of the Bugey, CDHS and KARMEN experiments. This likelihood function will be discussed in the next section and in Appendix B. For the treatment of parameters other than d_e and d_μ, which appear in the fitting procedure to the SBL experiments, see also Appendix B.

The physically allowed region $\mathcal{R}_d$ of d_e and d_μ is described by the inequalities

$$\mathcal{R}_d: \quad d_e \geq 0,\ d_\mu \geq 0 \ \text{ and } \ d_e + d_\mu \leq 1. \tag{28}$$

In order to incorporate it into our procedure, we define a function $R(d_e, d_\mu)$ such that $R(d_e, d_\mu) = 1$ for $(d_e, d_\mu) \in \mathcal{R}_d$ and 0 otherwise. This function has thus the task of a prior which confines (d_e, d_μ) to the physically meaningful region. Adopting the maximum likelihood method of Sect. 3.2 in order to deal with the parameters $A_{\rm ud}$ and $P_{\rm CH}$ and combining this method with (15), we finally arrive at the desired probability distribution

$$p_m(d_e, d_\mu) = \frac{L_{\rm osc}(d_e, d_\mu) L^m_{\rm ud}(d_e, d_\mu) L^m_{\rm CH}(d_e) R(d_e, d_\mu)}{\int {\rm d}d'_e \int {\rm d}d'_\mu L_{\rm osc}(d'_e, d'_\mu) L^m_{\rm ud}(d'_e, d'_\mu) L^m_{\rm CH}(d'_e) R(d'_e, d'_\mu)}. \quad (29)$$

The dependence of $L^m_{\rm ud}(d_e, d_\mu)$ and $L^m_{\rm CH}(d_e)$ on d_e and d_μ comes in through the substitutions (26) and (25) of the boundaries a and b.

Discussing now the Bayesian approach described in Sect. 3.1, we have the prior probability density

$$\pi(d_e, d_\mu, A_{\rm ud}, P_{\rm CH}) = \frac{1}{2} R(d_e, d_\mu) \pi_{\rm ud}(d_e, d_\mu, A_{\rm ud}) \pi_{\rm CH}(d_e, P_{\rm CH}). \quad (30)$$

We stress that

$$\int {\rm d}A_{\rm ud} \int {\rm d}P_{\rm CH} \pi(d_e, d_\mu, A_{\rm ud}, P_{\rm CH}) = \frac{1}{2} R(d_e, d_\mu) \quad (31)$$

is fulfilled. This equation tells us that, after integrating over the other variables, the prior probability density for d_e and d_μ is uniform. Since these are the variables whose distribution we want to calculate, (31) assures us that with our choice of priors we have not introduced a bias in the distribution of d_e and d_μ.

According to the Bayesian approach in Sect. 3.1 we perform the integrations

$$\int {\rm d}A_{\rm ud} \int {\rm d}P_{\rm CH} L_{\rm ud} L_{\rm CH} \pi. \quad (32)$$

Finally, we obtain via this method the probability distribution

$$p_b(d_e, d_\mu) = \frac{L_{\rm osc}(d_e, d_\mu) \ell_{\rm ud}(d_e, d_\mu) \ell_{\rm CH}(d_e) R(d_e, d_\mu)}{\int {\rm d}d'_e \int {\rm d}d'_\mu L_{\rm osc}(d'_e, d'_\mu) \ell_{\rm ud}(d'_e, d'_\mu) \ell_{\rm CH}(d'_e) R(d'_e, d'_\mu)}. \quad (33)$$

It is important to note that for every Δm^2 we have such a distribution. The SBL mass-squared difference, which is hidden in $L_{\rm osc}$, is not on the same footing as d_e and d_μ in our approach. For every given Δm^2, we find restrictions on d_e and d_μ from experiment[3] which allow us finally to obtain a bound on the transition amplitude $A_{\mu;e}$ for any given CL. Choosing a CL β, we find the corresponding bound on $A_{\mu;e}$ by the prescription

$$\int\limits_{4 d_e d_\mu \le A^0_\beta} {\rm d}d_e {\rm d}d_\mu p_j(d_e, d_\mu) = \beta \quad (j = m, b). \quad (34)$$

[3] Note that in the analyses of the Bugey [23] and CDHS [25] experiments Δm^2 is treated in the same way

For instance, if we choose $\beta = 0.99$, with (34) we can calculate a number $A^0_{0.99}$ such that $A_{\mu;e} \le A^0_{0.99}$ at 99% CL.

The two distributions $p_m(d_e, d_\mu)$ (29) and $p_b(d_e, d_\mu)$ (33) are, of course, different functions of the variables. The method to obtain bounds on $A_{\mu;e}$ as given by (34) is the same for both distributions. In the following, we will comment on how much the bounds on $A_{\mu;e}$ calculated with both distributions differ numerically.

4.2 A qualitative discussion of the SBL data

As mentioned previously, the SBL experiments are treated with the likelihood function

$$L_{\rm osc}(d_e, d_\mu) = L_{\rm Bugey}(d_e) \times L_{\rm CDHS}(d_\mu) \times L_{\rm KARMEN}(A_{\mu;e}), \quad (35)$$

which enters (27). Here we want to discuss some features of $L_{\rm osc}$ and how these features influence the bound on $A_{\mu;e}$. Let us start with the Bugey [23] and CDHS [25] experiments. Both are disappearance experiments and, therefore, the relevant SBL survival probabilities are given by

$$P_{\nu_\alpha \to \nu_\alpha} = P_{\bar\nu_\alpha \to \bar\nu_\alpha} = 1 - 4 d_\alpha (1 - d_\alpha) \sin^2 \frac{\Delta m^2 L}{4E}, \quad (36)$$

where $\alpha = e$ refers to the Bugey and $\alpha = \mu$ to the CDHS experiment. Both experiments have not found evidence for neutrino oscillations. In the case of the Bugey experiment the survival amplitude $4 d_e (1 - d_e)$ is bounded by 0.1 or smaller values in the relevant range $0.1\,{\rm eV}^2 \lesssim \Delta m^2 \lesssim 10\,{\rm eV}^2$ at 90% CL [23]. Thus, d_e is either very small or close to 1. Since for solar neutrinos the inequality

$$P^{\odot}_{\nu_e \to \nu_e} \ge d_e^2 \quad (37)$$

holds [8], d_e must be small[4] and in the fit of the Bugey data we make the approximation $d_e(1 - d_e) \simeq d_e$ in the survival probability. In principle, the inequality (37) should be included in our analysis with the help of one of the methods discussed in Sects. 3.1 and 3.2, but in view of the smallness of the Bugey survival amplitude this is not necessary. In the case of the CDHS experiment, for $\Delta m^2 \gtrsim 0.3\,{\rm eV}^2$, there is an analogous feature concerning d_μ [25]; there, the selection of the small d_μ is guaranteed by the up–down inequality (12) [10]. For smaller Δm^2 the CDHS restriction disappears and values of d_μ as large as 0.5 are allowed by the up–down inequality. Therefore, in $L_{\rm CDHS}$ we do not neglect d_μ^2 in the survival amplitude because this would not be justified.

In the KARMEN experiment, $\bar\nu_\mu \to \bar\nu_e$ transitions have not been observed and the KARMEN exclusion curve [26, 27] cuts right through the region allowed by LSND. Therefore, it is important to take into account the KARMEN result in our analysis. For the details of our fit to the

[4] We want to stress that this is the only place where solar neutrino data enter our analysis. Moreover, our inference that d_e must be small is independent of the actual solution to the solar neutrino problem

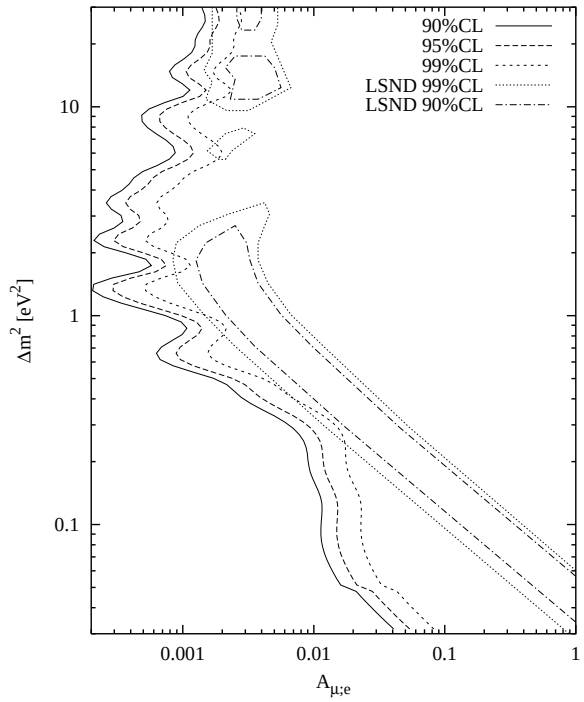

Fig. 1. Upper bounds on the transition amplitude $A_{\mu;e}$ in the case of (3+1)-mass spectra for 90%, 95% and 99% CL. These bounds have been calculated with the maximum likelihood approach for the inclusion of the atmospheric up–down inequality (12) and the CHOOZ inequality (23) as described in Sect. 3.2. Also shown are the regions allowed by the latest LSND results [6] at 90% and 99% CL

KARMEN data and the analogous details concerning the Bugey and CDHS experiments see Appendix B.

We include the CHOOZ result in our analysis for $\Delta m^2 \geq 0.05\,\mathrm{eV}^2$, where the bound on $\sin^2 2\theta$ in the CHOOZ plots is a straight line [22]; this guarantees that oscillations with the SBL Δm^2 are averaged out and hence (23) is valid. The CHOOZ result has an effect on the $A_{\mu;e}$ exclusion curve mainly for Δm^2 where the Bugey bound on d_e is not so strong, which is the case for Δm^2 around $0.1\,\mathrm{eV}^2$ and $\Delta m^2 \gtrsim 5\,\mathrm{eV}^2$.

4.3 The bound on $A_{\mu;e}$

Figure 1 represents the main result of this paper. In this figure we show the regions in the Δm^2–$A_{\mu;e}$ plane allowed by LSND at 90% and 99% CL [6] and our exclusion curves for $A_{\mu;e}$ with (3+1)-mass spectra at 90%, 95% and 99% CL. These exclusion curves have been calculated using the maximum likelihood approach of Sect. 3.2 for the treatment of the *true* values A_{ud} and P_{CH}. This method gives – for most values of Δm^2 – slightly weaker bounds than the Bayesian approach of Sect. 3.1; however, the numerical difference between the two methods is always smaller than 4%. We read off from Fig. 1 that the 99% CL LSND region has no overlap with the allowed region to the left of our 95% CL bound. This shows that the likelihood of (3+1)-mass spectra is not very high. Comparing the 99% CL exclusion curve with the 99% CL LSND region and confining ourselves to $\Delta m^2 < 10\,\mathrm{eV}^2$, we find overlaps at $\Delta m^2 \sim 6,\ 1.7,\ 0.9$ and approximately between 0.25 and $0.4\,\mathrm{eV}^2$. This agrees with the findings in [13], where 90% exclusion curves and the bound on $A_{\mu;e}$ derived in [8] are compared with the 99% CL LSND region. The result of the inclusion of the CHOOZ result for $\Delta m^2 \geq 0.05\,\mathrm{eV}^2$ can be seen as a jump in our exclusion curves. From this jump the effect of the CHOOZ result can be read off for small mass-squared differences. Let us stress once more that in our analysis an exclusion curve for a given CL is the result of a well-defined statistical procedure and is obtained by including all available data other than the LSND data; such exclusion curves have a precise statistical meaning; an overlap of the 99% CL LSND region with the region to the left of an exclusion curve occurs only with the exclusion curve at 99% CL, but not at 95% CL.

There are claims in the literature that all three indications in favour of neutrino oscillations are compatible with *three* neutrinos [29]. Such claims have been refuted by a combined fit to the data [30]. In our analysis we arrive at the same conclusion, because our treatment of the (3+1)-spectra is also applicable in the case of three neutrinos, where one has (2+1)-mass spectra, since there is a SBL mass-squared difference Δm^2 and another mass-squared difference much smaller than Δm^2; assuming that m_3 is the mass separated from the other two by the LSND mass gap, we have to make the identification $d_\alpha = |U_{\alpha 3}|^2$ ($\alpha = e, \mu$). The values of Δm^2 and $A_{\mu;e}$, indicated in the papers of [29] as preferred solutions, lie in the region allowed by LSND at 99% and thus beyond our 95% CL exclusion curve in Fig. 1.

5 The (2+2)-neutrino mass spectra

If we want to treat the (2+2)-neutrino mass spectra with the method discussed in the previous two sections, the situation is more involved. In this case the $\nu_\mu \to \nu_e$ transition amplitude is given by [8]

$$A_{\mu;e} = 4\left|\sum_{j=1,2} U_{ej}U_{\mu j}^*\right|^2 = 4\left|\sum_{j=3,4} U_{ej}U_{\mu j}^*\right|^2 \qquad (38)$$

and cannot be expressed by

$$d_\alpha = \sum_{j=3,4} |U_{\alpha j}|^2 \quad (\alpha = e, \mu), \qquad (39)$$

as in the case of the (3+1)-spectra (see (4)). This suggests to perform an analysis with the five parameters d_e, d_μ, $A_{\mu;e}$, A_{ud} and P_{CH} in the case of the (2+2)-spectra.

Let us explore in more detail the relationship between the amplitude $A_{\mu;e}$ and the parameters d_e and d_μ. From (38), using the Cauchy–Schwarz inequality, we readily obtain the inequality [8,31]

$$A_{\mu;e} \leq 4\min[d_e d_\mu, (1-d_e)(1-d_\mu)]. \qquad (40)$$

This inequality implies that for every $A_{\mu;e}$ the following region is allowed in the d_e–d_μ plane:

$$\mathcal{F}(A_{\mu;e}) : \begin{cases} \frac{1}{2}(1-\sqrt{1-A_{\mu;e}}) \leq d_e \leq \frac{1}{2}(1+\sqrt{1-A_{\mu;e}}), \\ A_{\mu;e}/4d_e \leq d_\mu \leq 1 - A_{\mu;e}/4(1-d_e). \end{cases} \tag{41}$$

For every $A_{\mu;e}$ between 0 and 1, this is a region in the unit square, confined by two hyperbolas. Let us label the neutrino masses such that $\Delta m^2_{21} = \Delta m^2_{\rm atm}$ and $\Delta m^2_{43} = \Delta m^2_{\rm solar}$. Then, with the definitions (39), (9) and (11) hold also for the (2+2)-mass spectra and we obtain the inequalities

$$-A_{\rm ud} \leq G'(d_e, d_\mu, A_{\mu;e}) = \frac{(1-d_\mu)^2 + A_{\mu;e}/4r}{(1-d_\mu)^2 + 2d_\mu^2 + 3A_{\mu;e}/4r} \tag{42}$$

and

$$A_{\rm ud} \leq H'(d_e, d_\mu, A_{\mu;e}) = \frac{d_\mu(1-d_\mu) - A_{\mu;e}/4r}{1 - d_\mu(1-d_\mu) + A_{\mu;e}/4r} \tag{43}$$

for the atmospheric up–down asymmetry. Furthermore, the survival probability for solar neutrinos is bounded by $P^{\odot}_{\nu_e\to\nu_e} \geq \frac{1}{2}(1-d_e)^2$. Therefore, d_e is close to one[5] and we make the approximation $d_e(1-d_e) \simeq 1-d_e$ in the Bugey survival amplitude. Note that the CHOOZ inequality (23) also holds for the (2+2)-spectra.

In analogy to (34) in the (3+1)-case, our aim is to obtain a probability distribution in $A_{\mu;e}$. Here we confine ourselves to the maximum likelihood method of Sect. 3.2 for the treatment of inequalities. In addition to the up–down and CHOOZ inequalities we have to take into account (41). According to the method of Sect. 3.2, we maximise with respect to $A_{\rm ud}$, $P_{\rm CH}$, d_e and d_μ. The maximization with respect to the first two variables leads to the functions $L'^m_{\rm ud}$ and $L^m_{\rm CH}$, which are defined in Sect. 3.3. The prime on the first function indicates that now it is obtained from $L^m_{\rm ud}$ by the replacement $G \to G'$ and $H \to H'$. Generalising the method of Sect. 3.2, we define

$$L'(A_{\mu;e}) = \max_{(d_e,d_\mu)\in\mathcal{F}(A_{\mu;e})} \left[L'_{\rm osc} L'^m_{\rm ud} L^m_{\rm CH} \right], \tag{44}$$

where $L'_{\rm osc}$ is given by (35), but in view of the appearance of $A_{\mu;e}$ in $L_{\rm KARMEN}$ it is interpreted as a function of three variables. Finally, we obtain the probability distribution for $A_{\mu;e}$ given by

$$p'_m(A_{\mu;e}) = \frac{L'(A_{\mu;e})\Theta(A_{\mu;e})\Theta(1-A_{\mu;e})}{\int \mathrm{d}A'_{\mu;e} L'(A'_{\mu;e})\Theta(A'_{\mu;e})\Theta(1-A'_{\mu;e})}. \tag{45}$$

In Fig. 2 the 90% CL bound on $A_{\mu;e}$ calculated with the distribution (45) is plotted. In this figure the 90% and 99% CL level regions of LSND are also depicted. The region to the left of the bound has an overlap area with the LSND region of 90% CL. This shows that the (2+2)-spectra are well compatible with all data. Also shown in Fig. 2 are the KARMEN and Bugey exclusion curves. As expected, for large Δm^2 the solid line of our exclusion curve follows rather well the KARMEN exclusion curve, whereas for small Δm^2 it tends to follow the Bugey curve. Due to the inclusion of the CHOOZ result above $0.05\,\mathrm{eV}^2$, the solid line is more restrictive there than the Bugey curve, whereas below $0.05\,\mathrm{eV}^2$ both curves are nearly identical. We have also investigated the exclusion curve of the (2+2)-spectra within the Bayesian approach to inequalities of Sect. 3.1. In this approach we have more freedom to make "reasonable" choices for priors than in the (3+1)-case, and, numerically, the $A_{\mu;e}$ bounds tend to be a little more restrictive than the solid line in Fig. 2.

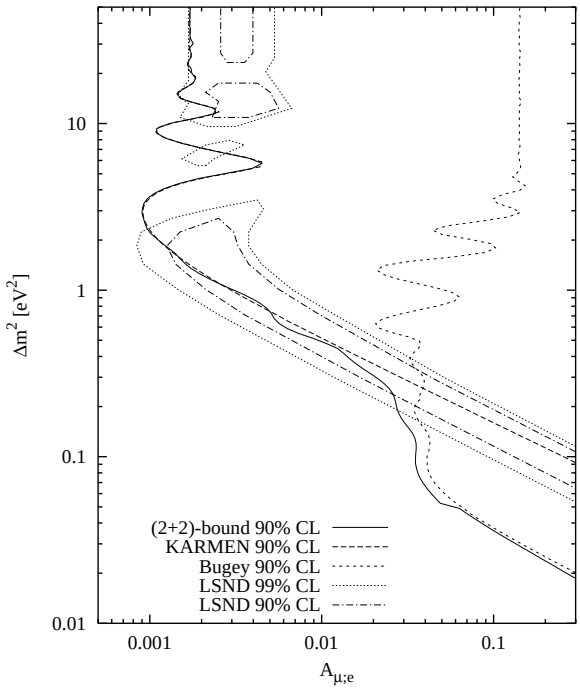

Fig. 2. The upper bound on the transition amplitude $A_{\mu;e}$ in the case of (2+2)-mass spectra for 90% CL calculated with the probability distribution (45). Also shown are the 90% and 99% CL level regions of LSND of [6], and the Bugey and KARMEN bounds referring to 90% CL as given by our reanalysis

6 Conclusions

In this paper we have examined the (3+1) and (2+2)-classes of the 4-neutrino mass spectra within a rigorous statistical analysis. Since we do not have sufficient information concerning the final LSND data [6], we have chosen the approach to analyse all other available data and compare our result with the LSND result in a Δm^2–$A_{\mu;e}$ plot. This approach suggests to extract that information from the solar and atmospheric data which is most relevant for SBL oscillations with respect to Δm^2. This extraction is most appropriately done in the form of inequalities involving elements of the neutrino mixing matrix [8–10]. Similarly, we have extracted the "SBL information" contained

[5] If d_e is small, then it follows that $P^{\odot}_{\nu_e\to\nu_e} \gtrsim 0.5$, which is in disagreement with the result of the Homestake experiment (see first paper in [2]); moreover, for small d_e we obtain the same bound on $A_{\mu;e}$ as for the disfavoured (3+1)-mass spectra

in the CHOOZ result. On the other hand, concerning the SBL experiments, we have fully included the data of the Bugey, CDHS and KARMEN experiments.

Since our aim has been to incorporate in the statistical analysis the atmospheric up–down inequality, (12) or (42), and the CHOOZ inequality (23), we have made use of the likelihood function in combination with the Bayesian approach to probability which allows us to derive probability distributions of the parameters which are to be estimated. In this context we have presented two possibilities for including inequalities involving parameters: one way is to treat them in the form of prior probability densities for which a "reasonable choice" has to be made; another way is a kind of maximum likelihood treatment. Numerically, we have compared both methods for exclusion curves in the case of the (3+1)-spectra and found that the difference is negligible.

With the method described in this paper we have obtained for every Δm^2 a probability distribution for the SBL transition amplitude $A_{\mu;e}$, from which we could derive bounds as a function of Δm^2 on this amplitude for any CL. The results are shown in Figs. 1 and 2 for the (3+1) and (2+2)-neutrino mass spectra, respectively. In the latter case our 90% CL exclusion curve is close to the KARMEN exclusion curve down to $\Delta m^2 \sim 0.5\,\mathrm{eV}^2$; there it turns off and starts to come close to the exclusion curve given by the Bugey data. Thus, for the (2+2)-spectra our method reproduces more or less what one obtains by naively comparing the KARMEN and Bugey exclusion curves with the region allowed by LSND. Therefore, these spectra are well compatible with all the data. On the other hand, in the case of the (3+1)-spectra, our 95% CL bound has no overlap with the LSND region of 99% CL. We, therefore, come to the conclusion that this spectral class is rather unlikely, even with the recent change in the LSND region.

Thus we strengthen with the method presented here the claims made in [8–10]. Should the LSND result be confirmed by the MiniBooNE Collaboration [32], then, in a 4-neutrino scheme, the sterile neutrino should make its appearance either in the solar or atmospheric neutrinos, or both.

Acknowledgements. We thank C. Giunti and S.M. Bilenky for many useful discussions. We are very grateful to F. Dydak and J. Wotschack for valuable information about the CDHS experiment and to C. Walter for providing us with the latest results of the Super-Kamiokande up–down asymmetry. T.S. is supported by the Austrian Academy of Sciences.

Appendix

A The relationship between the Bayesian and the maximum likelihood methods for the treatment of inequalities

Here we want to elucidate the relationship between the methods for the inclusion of inequalities introduced in Sects. 3.1 and 3.2. In the Bayesian approach to this problem we consider in general integrals of the type

$$I[\pi] = \int_a^b \mathrm{d}z L_Z(z)\pi(z), \tag{46}$$

where L_Z is given by (16). A prior π is a positive and piecewise continuous function such that $\int_a^b \mathrm{d}z\pi(z) = 1$. In Sect. 3.1 we have used the flat prior (18). If we denote the set of all prior probability densities on the interval $[a, b]$ by $\mathcal{P}$, then the following proposition holds.

Proposition: For the integral in (46) one has the upper limit

$$\max_{\pi\in\mathcal{P}} I[\pi] = L_Z^m, \tag{47}$$

where L_Z^m is given by (22).

Proof: The proof is very straightforward. Let us first assume that $z_{\mathrm{exp}} > b$. Then we have

$$I[\pi] < L_Z(b)\int_a^b \mathrm{d}z\pi(z) = L_Z(b).$$

Thus we have found an upper bound on I. If we can find a sequence of π_k of prior probability densities such that

$$\lim_{k\to\infty} I[\pi_k] = L_Z(b),$$

then the proposition is proven for the case $z_{\mathrm{exp}} > b$. Such a sequence is easy to give: any sequence π_k, for which $\pi_k(z) = 0$ for $z \le b - 1/k$ holds, fulfills our purpose. For $z_{\mathrm{exp}} < a$ we proceed analogously. If $z_{\mathrm{exp}} \in [a, b]$, the upper bound on I is $L_Z(z_{\mathrm{exp}})$. The sequence π_k is constructed accordingly with the idea given before. Thus for the three cases $z_{\mathrm{exp}} > b$, $z_{\mathrm{exp}} < a$ and $z_{\mathrm{exp}} \in [a, b]$ we have the upper limits $L_Z(b)$, $L_Z(a)$ and $L_Z(z_{\mathrm{exp}})$, respectively. In summary, we just have obtained the expression (22). Q.E.D.

Thus the expression L_Z^m is obtained from the Bayesian approach as the maximum over all possible priors. Roughly speaking, the prior in I, which gives L_Z^m, is a delta function ($\delta(z-b)$, $\delta(z-a)$ or $\delta(z-z_{\mathrm{exp}})$); however, in order to choose the correct delta function one has to know the experimental value z_{exp} and, therefore, such a function does not deserve the name "prior" anymore. Though $\ell_Z < L_Z^m$ holds, it is not obvious which method gives the stronger constraint in an actual situation, because one has additional factors in the probability distribution one aims at, coming from additional data, and one has to normalise the combined distribution (see (15)). Moreover, the bounds a and b are in general functions of the parameters whose distribution we want to know. In the concrete situation discussed in Sect. 4 the maximum likelihood method represented by L_Z^m gives a slightly weaker restriction on the transition amplitude $A_{\mu;e}$ for most Δm^2.

B The analyses of the Bugey, CDHS and KARMEN experiments

In this appendix we describe how the data of the SBL experiments Bugey, CDHS and KARMEN is included in

our analysis. We use as much information as can be recovered from the publications of the experimental groups to perform a fit to the data. The fact that we can reproduce the published 90% CL bounds in the case of 2-neutrino oscillations to a good accuracy inspires confidence in our analysis.

B.1 Bugey

The Bugey experiment [23] searches for $\bar{\nu}_e$ disappearance at the three distances 15 m, 40 m and 95 m away from a nuclear reactor. The electron antineutrinos are detected through the reaction $\bar{\nu}_e + p \to e^+ + n$. As input data for our analysis we use Fig. 17 of [23], where the ratios of the observed events to the number of expected events in case of no oscillations are shown for the three positions in bins of positron kinetic energy in the range $1\,\mathrm{MeV} \leq E_{e^+} \leq 6\,\mathrm{MeV}$.

For the analysis we follow (9) of [23] and use the χ^2-function

$$\chi^2 = \sum_j \left\{ \sum_{i=1}^{N_j} \frac{\left[(Aa_j + b(E_{ji} - E_0))R_{ji}^{\mathrm{theo}} - R_{ji}^{\mathrm{exp}}\right]^2}{\sigma_{ji}^2} + \frac{(a_j - 1)^2}{\sigma_a^2} \right\} + \frac{(A-1)^2}{\sigma_A^2} + \frac{b^2}{\sigma_b^2}. \quad (48)$$

Here $j = 15, 40, 95$ labels the three positions, i the positron energy bins and $N_{15} = N_{40} = 25$, $N_{95} = 10$ are the numbers of bins at each position. For E_{ji} we take the mean positron energy in bin ji. R_{ji}^{exp} is the ratio of measured to expected events in each bin with its statistical error σ_{ji}, both read off from Fig. 17 of [23]. R_{ji}^{theo} is the theoretical prediction for this ratio in the case of oscillations, depending on the oscillation parameters, and we set $R_{ji}^{\mathrm{theo}} = \langle P_{\bar{\nu}_e \to \bar{\nu}_e} \rangle_{ji}$, where $P_{\bar{\nu}_e \to \bar{\nu}_e}$ is given in (36). Various systematic uncertainties are taken into account by minimising the χ^2, (48), with respect to the five parameters A, a_j and b for given oscillation parameters. In [23] the values $\sigma_A = 4.796\%$, $\sigma_a = 1.414\%$, $\sigma_b = 0.02\,\mathrm{MeV}^{-1}$ and $E_0 = 1\,\mathrm{MeV}$ are given.

To perform the averaging of the survival probability we estimate the uncertainty in the flight length of the neutrinos because of the size of the production region and the detector to 3 m and we assume that the flux varies with the distance as L^{-2}. In the relevant energy range antineutrino and positron energy are related by $E_\nu = E_{e^+} + 1.8\,\mathrm{MeV}$ to a very good approximation. For the purpose of averaging the survival probability over the energy range in one bin it is a good approximation to take neutrino flux, detection cross section and efficiency as constant with energy. The reason for this is that the energy bins are relatively small and only ratios of observed to expected events in each bin are considered. Furthermore, we assume a Gaussian resolution function for the positron energy measurement with variance 0.4 MeV.

The likelihood function in (35) which contains the information of the Bugey experiment is obtained from the χ^2 of (48) by [21]

$$L_{\mathrm{Bugey}}(d_e) \propto \exp\left(-\frac{1}{2}\chi^2\right). \quad (49)$$

The 90% CL bound on d_e obtained from this likelihood function alone can be compared to the Bugey exclusion curve in the 2-neutrino case with the identification $\sin^2 2\theta_{\mathrm{Bugey}} \simeq 4d_e$. The curve obtained by our analysis is shown in Fig. 2 and compares well with the originally published one [23].

In (36) contributions of oscillations because of $\Delta m^2_{\mathrm{atm}}$ to the SBL disappearance amplitude are neglected. This approximation may not be exactly fulfilled in the Bugey experiment for small $\Delta m^2_{\mathrm{SBL}}$ and large $\Delta m^2_{\mathrm{atm}}$. We have calculated the 90% CL bound from Bugey by taking into account also oscillations with $\Delta m^2_{\mathrm{atm}} = 6 \times 10^{-3}\,\mathrm{eV}^2$, which is the 99% CL upper bound on $\Delta m^2_{\mathrm{atm}}$ [15], and find that for $\Delta m^2_{\mathrm{SBL}} > 0.04\,\mathrm{eV}^2$ the effect is smaller than 6%.

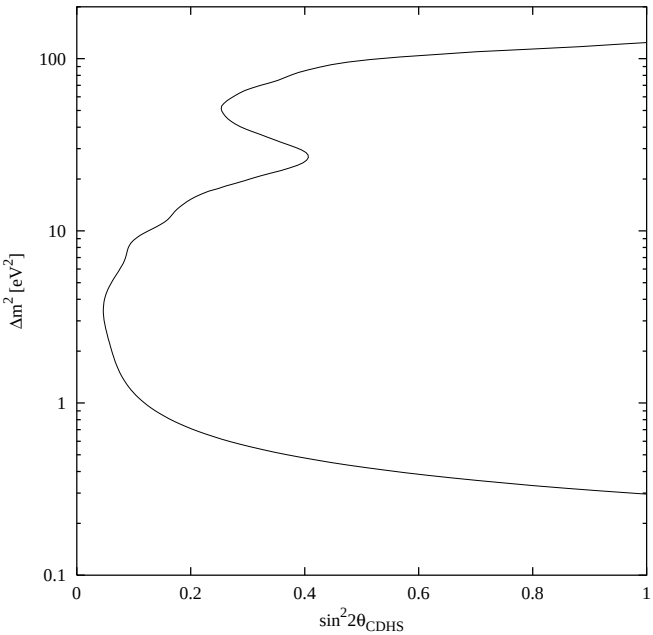

Fig. 3. The 90% CL bound on $\sin^2 2\theta_{\mathrm{CDHS}}$ given by our reanalysis of the CDHS experiment as described in Sect. B.2

B.2 CDHS

The CDHS experiment [25] searches for ν_μ disappearance by comparing the number of events in the so-called back and front detectors at the distances $L_{\mathrm{back}} = 885\,\mathrm{m}$ and $L_{\mathrm{front}} = 130\,\mathrm{m}$, respectively, from the neutrino source. The neutrinos are detected via muons produced in charged-current interactions. The data are given in the form of the double ratios

$$R_{\mathrm{corr}} = \frac{N_{\mathrm{back}}/N_{\mathrm{front}}}{N_{\mathrm{back}}^{\mathrm{MC}}/N_{\mathrm{front}}^{\mathrm{MC}}}, \quad (50)$$

where N_{back} (N_{front}) is the number of observed events in the back (front) detector and $N_{\mathrm{back}}^{\mathrm{MC}}$ and $N_{\mathrm{front}}^{\mathrm{MC}}$ are the

corresponding quantities expected for no oscillations calculated by Monte Carlo.

The ratios (50) are given in 15 bins of "projected range in iron". This is the distance traveled by the muon in the detector (consisting of iron) projected onto the detector axis, which has an angle of 22° relative to the neutrino beam axis. We calculate the range in iron $r(E_\mu)$ of a muon with energy E_μ by integrating (23.1) of [21]. The muon energy intervals $[E_\mu^{(i1)}, E_\mu^{(i2)}]$ corresponding to the intervals of projected range ($r_{\rm proj}$) for bin i given in Table 1 of [25] are obtained by applying the relation $r_{\rm proj}(E_\mu) \simeq r(E_\mu)\cos\vartheta\cos 22^\circ$, where $\vartheta \simeq 20^\circ$ is the average scattering angle of the muons [33].

We estimate the number of events in bin i and at position $p =$ back or front using

$$N_{ip} \propto M_p \int_{E_\mu^{(i1)}}^{E_\mu^{(i2)}} {\rm d}E_\mu \int_{E_\mu}^{\infty} {\rm d}E_\nu \int_{L_p-\Delta L_p/2}^{L_p+\Delta L_p/2} {\rm d}L L^{-2} \times P_{\nu_\mu\to\nu_\mu}(L/E_\nu) \times \Phi(E_\nu) \frac{{\rm d}\sigma_{\rm DIS}(E_\nu, E_\mu)}{{\rm d}E_\mu}. \quad (51)$$

Here M_p is the detector mass at position p. Taking into account the size of the decay tunnel (52 m) and the length relevant for detection in the back/front detector (72 m/ 22 m) [25] we have $\Delta L_{\rm back} = 52 + 72\,{\rm m}$ and $\Delta L_{\rm front} = 52 + 22\,{\rm m}$. The disappearance probability $P_{\nu_\mu\to\nu_\mu}(L/E_\nu)$ depending on the oscillation parameters is given in (36) and $\sigma_{\rm DIS}$ is the cross section for the deep inelastic scattering process $\nu_\mu + N \to \mu + X$ (see, e.g., [34]). The neutrino flux $\Phi(E_\nu)$ in the relevant neutrino energy range $E_\nu \gtrsim 0.7\,{\rm GeV}$ is proportional to $\exp(-E_\nu/1\,{\rm GeV})$ [25, 33]. Finally, we obtain for the theoretical prediction for the double ratios (50) in bin i

$$R^i_{\rm theo} = \frac{N_{i\rm back}}{N_{i\rm front}} \left(\frac{L_{\rm back}}{L_{\rm front}}\right)^2 \frac{M_{\rm front}}{M_{\rm back}}, \quad (52)$$

and we define the CDHS likelihood function by

$$L_{\rm CDHS}(d_\mu) \propto \exp\left[-\frac{1}{2}\sum_{ij}(R^i_{\rm corr} - R^i_{\rm theo})(S^{-1})_{ij}(R^j_{\rm corr} - R^j_{\rm theo})\right]. \quad (53)$$

Assuming total correlation between any two bins, the covariance matrix is given by $S_{ij} = \delta_{ij}\sigma_i^2 + \sigma_{\rm syst}^2$. $R^i_{\rm corr}$ and its statistical error σ_i are read off from Table 1 of [25]. The overall systematic error in the ratio of event rates in the two detectors was estimated to $\sigma_{\rm syst} = 2.5\%$ in [25].

The 90% CL bound on $\sin^2 2\theta_{\rm CDHS} = 4d_\mu(1-d_\mu)$ obtained by our analysis is shown in Fig. 3. It is very similar to the bound published by the CDHS collaboration [25]. There are minor differences for small mass squared differences, which could have some effect for our bound on $A_{\mu;e}$ in the region $0.2\,{\rm eV}^2 \lesssim \Delta m^2 \lesssim 0.4\,{\rm eV}^2$: our bound disappears at $\Delta m^2 \simeq 0.3\,{\rm eV}^2$, whereas the CDHS bound extends down to approximately $0.24\,{\rm eV}^2$.

B.3 KARMEN

The latest data of the $\bar\nu_\mu \to \bar\nu_e$ oscillation search in the KARMEN experiment is presented in [27]. Analysing the data taken from February 1997 to March 2000 they find a total of 11 candidate events, in good agreement with the expected number of background events for no oscillations of 12.3 ± 0.6. For our analysis we use the data resulting from the detection process $\bar\nu_e + p \to e^+ + n$. The positron spectrum $S(E_{e^+})$ expected for $A_{\mu;e} \equiv \sin^2 2\theta_{\rm KARMEN} = 1$ and $\Delta m^2 = 100\,{\rm eV}^2$ we take from Fig. 2(a) of [26]. To estimate the number of events in a positron energy interval $[E_1, E_2]$ resulting from neutrino oscillations we follow (B1) of [35]:

$$N^{\rm osc} = N \int_{E_1}^{E_2} {\rm d}E_{e^+} S(E_{e^+}) \int_{L_1}^{L_2} {\rm d}L L^{-2} P_{\bar\nu_\mu\to\bar\nu_e}(L/E_\nu), \quad (54)$$

where the oscillation probability $P_{\bar\nu_\mu\to\bar\nu_e}$ is given in (3). For $L_{1,2}$ we take $17.5 \mp 1.75\,{\rm m}$ [35] and antineutrino energy and positron kinetic energy are related by $E_\nu = E_{e^+} + 1.8\,{\rm MeV}$. The normalization factor N is fixed by requiring that for the total positron energy range $E_1 = 16\,{\rm MeV}$, $E_2 = 52\,{\rm MeV}$, full mixing ($\sin^2 2\theta_{\rm KARMEN} = 1$) and $\Delta m^2 \geq 100\,{\rm eV}^2$ the number of events resulting from oscillations is 2442 (see Table 1 of [27]).

From Fig. 2(b) of [27] we read off for each of the 9 positron energy bins the number of observed events $N_i^{\rm obs}$ and the number of background events expected for no oscillations B_i. Then we construct the likelihood function by using the Poisson distribution:

$$L_{\rm KARMEN}(A_{\mu;e}) = \prod_{i=1}^{9} \frac{1}{N_i^{\rm obs}!}(N_i^{\rm osc} + B_i)^{N_i^{\rm obs}} {\rm e}^{-(N_i^{\rm osc}+B_i)}. \quad (55)$$

Here $N_i^{\rm osc}$ is calculated from (54) by choosing E_1 and E_2 according to the bin i. The 90% CL bound on $A_{\mu;e}$ for a given Δm^2 obtained from the probability distribution implied by (55) in the Bayesian approach is shown in Fig. 2. Our bound is very close to the one presented in [27].

References

1. S.M. Bilenky, B. Pontecorvo, Phys. Rep. **41**, 225 (1978)
2. B.T. Cleveland et al., Astrophys. J. **496**, 505 (1998); K.S. Hirata et al., Kamiokande Coll., Phys. Rev. Lett. **77**, 1683 (1996); W. Hampel et al., GALLEX Coll., Phys. Lett. B **447**, 127 (1999); D.N. Abdurashitov et al., SAGE Coll., Phys. Rev. Lett. **83**, 4686 (1999); Y. Fukuda et al., Super-Kamiokande Coll., Phys. Rev. Lett. **81**, 1158 (1998)
3. Y. Fukuda et al., Super-Kamiokande Coll., Phys. Rev. Lett. **81**, 1562 (1998)
4. Y. Fukuda et al., Kamiokande Coll., Phys. Lett. B **335**, 237 (1994); R. Becker-Szendy et al., IMB Coll., Nucl. Phys. B (Proc. Suppl.) **38**, 331 (1995); W.W.M. Allison et al., Soudan Coll., Phys. Lett. B **449**, 137 (1999); M. Ambrosio et al., MACRO Coll., Phys. Lett. B **434**, 451 (1998)

5. C. Athanassopoulos et al., LSND Coll., Phys. Rev. Lett. **77**, 3082 (1996); ibid. **81**, 1774 (1998)
6. G. Mills, LSND Coll., Talk given at Neutrino 2000, 15–21 June 2000, Sudbury, Canada, transparencies available at http://nu2000.sno.laurentian.ca
7. J.T. Peltoniemi, D. Tommasini, J.W.F. Valle, Phys. Lett. B **298**, 383 (1993); J.T. Peltoniemi, J.W.F. Valle, Nucl. Phys. B **406**, 409 (1993); D.O. Caldwell, R.N. Mohapatra, Phys. Rev. D **48**, 3259 (1993); E. Ma, P. Roy, ibid. **52**, R4780 (1995); E.J. Chun et al., Phys. Lett. B **357**, 608 (1995); J.J. Gomez-Cadenas, M.C. Gonzalez-Garcia, Z. Phys. C **71**, 443 (1996); E. Ma, Mod. Phys. Lett. A **11**, 1893 (1996); S. Goswami, Phys. Rev. D **55**, 2931 (1997)
8. S.M. Bilkenky, C. Giunti, W. Grimus, in Proceedings of Neutrino '96, Helsinki, Finland, 13–19 June 1996, p. 174, edited by K. Enqvist, K. Huitu, J. Maalampi (World Scientific, Singapore 1997); S.M. Bilenky, C. Giunti, W. Grimus, Eur. Phys. J. C **1**, 247 (1998)
9. N. Okada, O. Yasuda, Int. J. Mod. Phys. A **12**, 3669 (1997)
10. S.M. Bilenky, C. Giunti, W. Grimus, T. Schwetz, Phys. Rev. D **60**, 073007 (1999)
11. V. Barger et al., Phys. Lett. B **489**, 345 (2000)
12. V. Barger, S. Pakvasa, T.J. Weiler, K. Whisnant, Phys. Rev. D **58**, 093016 (1998)
13. C. Giunti, M. Laveder, hep-ph/0010009
14. O.L.G. Peres, A.Yu. Smirnov, hep-ph/0011054
15. H. Sobel, Super-Kamiokande Coll., Talk given at Neutrino 2000, 15–21 June 2000, Sudbury, Canada, transparencies available at http://nu2000.sno.laurentian.ca
16. Y. Suzuki, Super-Kamiokande Coll., Talk given at Neutrino 2000, 15–21 June 2000, Sudbury, Canada, transparencies available at http://nu2000.sno.laurentian.ca
17. M.C. Gonzalez-Garcia, C. Peña-Garay, hep-ph/0009041
18. D. Dooling, C. Giunti, K. Kang, C.W. Kim, Phys. Rev. D **61**, 073011 (2000); C. Giunti, M.C. Gonzalez-Garcia, C. Peña-Garay, Phys. Rev. D **62**, 013005 (2000); M.C. Gonzalez-Garcia, C. Peña-Garay, hep-ph/0011245
19. G.L. Fogli, E. Lisi, A. Marrone, hep-ph/0009299
20. G. Cowan, Statistical data analysis (Oxford University Press, New York 1998); B.P. Roe, Probability and statistics in experimental physics (Springer, New York 1992); G. Cowan, in Present and Future CP Measurements, p. 98, hep-ph/0102159
21. D.E. Groom et al., Particle Data Group, Eur. Phys. J. C **15**, 1 (2000)
22. M. Apollonio et al., CHOOZ Coll., Phys. Lett. B **466**, 415 (1999)
23. B. Achkar et al., Nucl. Phys. B **434**, 503 (1995)
24. S.M. Bilenky, A. Bottino, C. Giunti, C.W. Kim, Phys. Rev. D **54**, 1881 (1996); S.M. Bilenky, C. Giunti, C.W. Kim, S.T. Petcov, Phys. Rev. D **54**, 4432 (1996)
25. F. Dydak et al., Phys. Lett. B **134**, 281 (1984)
26. K. Eitel, B. Zeitnitz, KARMEN Coll., in Proceedings of Neutrino '98, Takayama, Japan, 4–9 June 1998, Nucl. Phys. Proc. Suppl. **77**, 212 (1999)
27. K. Eitel, KARMEN Coll., Talk given at Neutrino 2000, 15–21 June 2000, Sudbury, Canada, hep-ex/0008002
28. C. Walter, Super-Kamiokande Coll. (private communication)
29. R.P. Thun, S. McKee, Phys. Lett. B **439**, 123 (1998); G. Barenboim, F. Scheck, Phys. Lett. B **440**, 332 (1998); T. Ohlsson, H. Snellman, Phys. Rev. D **60**, 093007 (1999); G. Conforto et al., Phys. Lett. B **447**, 122 (1999); O. Haug, A. Faessler, J.D. Vergados, hep-ph/0005068
30. G.L. Fogli, E. Lisi, A. Marrone, G. Scioscia, hep-ph/9906450
31. S.M. Bilenky, C. Giunti, W. Grimus, Phys. Rev. D **57**, 1920 (1998)
32. A. Bazarko, MiniBooNE Coll., Talk given at Neutrino 2000, 15–21 June 2000, Sudbury, Canada, transparencies available at http://nu2000.sno.laurentian.ca
33. J. Wotschack (private communication)
34. S.M. Bilenky, Introduction to Feyman diagrams and electroweak interaction physics (Edition Frontière, Gif-sur-Yvette 1994)
35. G.L. Fogli, E. Lisi, G. Scioscia, Phys. Rev. D **56**, 3081 (1997)